JOURNAL OF GEOPHYSICAL RESEARCH, VOL. 92, NO. A5, PAGES 4740–4744, MAY 1, 1987

Ion Beams and the Ion/Ion Acoustic Instability Upstream From the Earth's Bow Shock

S. A. FUSELIER,[1] S. PETER GARY, M. F. THOMSEN, AND S. J. BAME

Earth and Space Science Division, Los Alamos National Laboratory, Los Alamos, New Mexico

D. A. GURNETT

Department of Physics and Astronomy, University of Iowa, Iowa City

This paper considers the generation of enhanced ion acoustic fluctuations by field-aligned ion beams upstream from the earth's bow shock. Steep slopes in the beam distribution parallel and possibly strongly oblique to the magnetic field are correlated with bursts of ion acoustic noise in the upstream region. Linear theory shows that it is the slope of the beam distribution at oblique angles to the magnetic field that determines the growth rate of the ion/ion acoustic instabilty. Because of instrument limitations we suggest but cannot confirm that enhanced ion acoustic fluctuations in the upstream region and in the presence of field-aligned beams are driven by such steep-sided distributions.

INTRODUCTION

Enhanced electrostatic fluctuations near the (Doppler shifted) ion plasma frequency are observed in many different space plasma environments: the solar wind [*Gurnett and Anderson*, 1977; *Gurnett et al.*, 1979*a*], upstream from the earth's bow shock [*Scarf et al.*, 1970; *Gurnett and Frank*, 1978], within the earth's bow shock and at other planetary bow shocks [*Gurnett*, 1985, and references therein], in the terrestrial magnetosheath [*Rodriguez*, 1979], in the plasma sheet boundary layer [*Grabbe and Eastman*, 1984], near slow shocks in the earth's distant magnetotail [*Scarf et al.*, 1984], at interplanetary shocks [*Gurnett et al.*, 1979*b*; *Kennel et al.*, 1982], and near comets [*Scarf et al.*, 1986; *Grard et al.*, 1986].

Although these fluctuations have been widely observed and often identified as being in the ion acoustic mode [e.g., *Fuselier and Gurnett*, 1984], the sources of free energy which drive these waves to the observed large amplitudes have not been identified in many cases. The basic problem is that although both electron-ion and ion-ion relative drifts can lead to unstable ion acoustic modes, linear kinetic theory based on drifting Maxwellian distributions shows that both instabilities typically require $T_e \gg T_i$ for significant growth at modest free energies. Since T_e is approximately equal to T_i in many environments where enhanced ion acoustic fluctuations are observed, it appears that non-Maxwellian properties of the distribution functions are necessary to explain many of these observations. For example, flat-topped electron distributions permit the electron/ion acoustic [*Thomsen et al.*, 1983] and the ion/ion acoustic [*Akimoto and Winske*, 1985] instabilities to grow at the terrestrial bow shock, and very cold ion beams are necessary for growth of the ion/ion acoustic instability at oblique propagation in the plasma sheet boundary layer [*Grabbe*, 1985; *Omidi*, 1985]. (Note that we here follow the terminology of *Gary and Omidi* [1986], which denotes the ion acoustic mode driven unstable by a relative ion-ion drift as the ion/ion acoustic instability and the same mode driven unstable by a relative electron-ion drift as the electron/ion acoustic instability.)

In this paper we address the particular issue of enhanced electrostatic fluctuations near the ion plasma frequency upstream from the terrestrial bow shock. Such waves were first identified as associated with ion beams by *Scarf et al.* [1970]; this association has also been demonstrated by *Gurnett and Frank* [1978] and *Anderson et al.* [1981]. *Gurnett and Frank* [1978] suggested that these fluctuations were short-wavelength ($\lambda \sim 2\pi\lambda_{De}$, where λ_{De} is the electron Debye length) ion acoustic waves Doppler-shifted by the motion of the solar wind from near the ion plasma frequency ($\sim$500 Hz in the solar wind) to frequencies between 1 and 10 kHz. Later, this suggestion was confirmed by *Fuselier and Gurnett* [1984], who showed that wavelengths inferred from antenna interference pattern effects were consistent with the ion acoustic dispersion relation. Fuselier and Gurnett also showed that these ion acoustic waves propagate generally away from the shock and at oblique angles (between 10° and 80°) to the magnetic field.

The association with backstreaming ions and oblique propagation strongly suggests that these waves are generated by the ion/ion acoustic instability. As far as we know, this is the only electrostatic short-wavelength instability that will grow at oblique angles to the magnetic field [*Gary and Omidi*, 1986]. However, to our knowledge, no measured distribution in the upstream region has ever been identified as clearly unstable to this instability. Indeed, for typical upstream conditions (beam density n_b about a few percent of the background ion density, electron to ion core temperature ratio $T_e/T_c \simeq 2$, and large beam temperatures $T_b/T_c \sim 10$–100), linear calculations with drifting Maxwellian distributions show that ion acoustic waves should be stable [*Gary and Omidi*, 1986].

This paper reconsiders the generation of ion acoustic instabilities by ion beams in the upstream region. Specifically, we examine the case of the relatively cold field-aligned ion beams [e.g., *Thomsen*, 1985, Figure 1]. Observations described here show that the correlation between ion beams and ion acoustic

[1]Now at Lockheed Palo Alto Research Laboratory, Palo Alto, California.

Paper number 6A8725.
0148-0227/87/006A-8725$02.00

waves is good only on coarse time scales. On fine time scales, this correlation breaks down, suggesting that details of the ion distribution and not the mere presence of suprathermal ions determine stability properties of the ion acoustic mode. Specifically, we argue that instability depends on the steepness of the slope of the beam distribution in the directions oblique to the magnetic field. Our observations indicate that the effective perpendicular beam temperature at the edge of the distribution may indeed be much colder than the perpendicular temperature obtained by integration over the beam velocity distribution. Since a colder perpendicular temperature reduces the ion/ion acoustic instability threshold in linear theory, we suggest that the non-Maxwellian steep sides of the beam distribution permit instability growth in spite of the large value of the integrated beam temperature.

INSTRUMENTATION

Ion data in this paper are from the Los Alamos/Garching fast plasma experiment (FPE) on ISEE 2 [*Bame et al.*, 1978]. The FPE measures a two-dimensional ion distribution (16 energies × 16 angles spaced 22.5° apart in azimuth) in 3 s, and the measurement is repeated every 3 s in high data rate. Solar wind ion measurements are from a separate solar wind instrument on ISEE 1 [*Bame et al.*, 1978]. Plasma wave observations are from the University of Iowa plasma wave instrument on ISEE 2 [*Gurnett et al.*, 1978]. This instrument measures the fluctuating electric fields in 16 logarithmically spaced frequency channels from 5.6 Hz to 31.1 kHz four times a second in high data rate.

OBSERVATIONS

Figure 1 shows the ion beam density and the electric field spectrum from 311 Hz to 31.1 kHz versus time for an upstream ion beam event on November 7, 1977. During this event the solar wind core ion and electron temperature and density were $T_c = 1.9 \times 10^4$ °K, $T_e = 1.2 \times 10^5$ °K, and $n_i = n_e = 13$ cm^{-3}. Note that for this event, $T_e/T_c = 6.3$, which is a factor of 3 larger than the "typical" solar wind ratio. Since an increase in T_e/T_c results in a decrease in the threshold of the ion/ion acoustic instability [*Gary and Omidi*, 1986], the possibility of generation of ion acoustic fluctuations is enhanced over typical solar wind conditions. Although suprathermal ions are present throughout the 10-min interval in Figure 1, below approximately 0.02 cm^{-3} we have no confidence in the measured beam densities. Plasma waves in the 31.1-kHz channel are electron plasma oscillations at the local electron plasma frequency (32 kHz) generated by electron beams in the upstream region [*Scarf et al.*, 1971]. Fluctuations between 311 Hz and 10 kHz are Doppler-shifted ion acoustic waves [*Fuselier and Gurnett*, 1984].

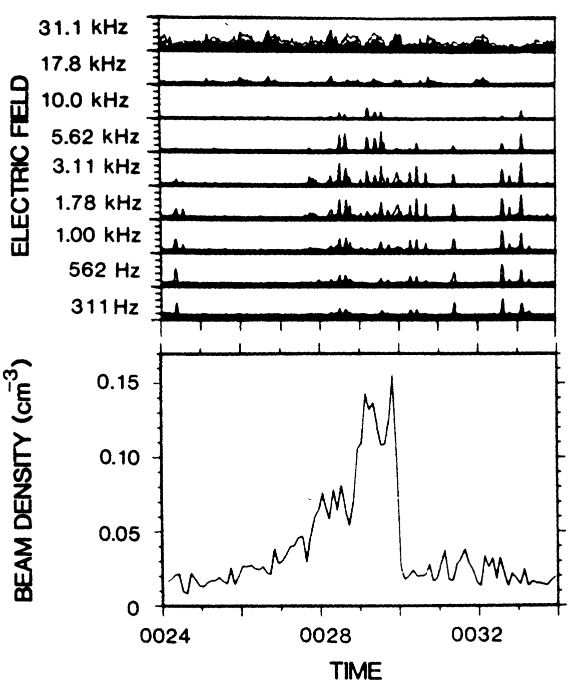

Fig. 1. Plasma wave intensity and ion beam density versus time for an ion beam event on November 7, 1977. Enhanced ion acoustic fluctuations (between 311 Hz and 10 kHz) are generally associated with larger ion beam densities. However, on fine time scales the ion acoustic fluctuations are bursty and not well correlated with beam density changes. Also, there are field-aligned beams present throughout the interval, yet there are several periods of no ion acoustic activity.

There is a general correlation between increased ion acoustic activity and increased ion beam density in Figure 1. However, on fine time scales the ion acoustic fluctuations are bursty and clearly not well correlated with beam density changes. Despite the large T_e/T_c ratio and despite the fact that there are suprathermal ions present throughout the interval in Figure 1, there are several periods of no ion acoustic wave activity (for example from 0026 to 0027 UT). Clearly, the mere presence of suprathermal ions does not guarantee the existence of ion acoustic waves. The bursty nature of the waves and the lack of correlation with beam density changes on fine time scales suggest that details of the ion distribution are crucial in determining instability of the ion acoustic mode. Other upstream ion events not shown here demonstrate this same lack of fine time scale correlation between the ion acoustic fluctuations and the ions beams.

In Figure 2, two 3-s snapshots of the ion distribution during the event shown in Figure 1 show details that may be important for the ion/ion acoustic instability. This figure shows contours of constant ion phase space density in two-dimensional

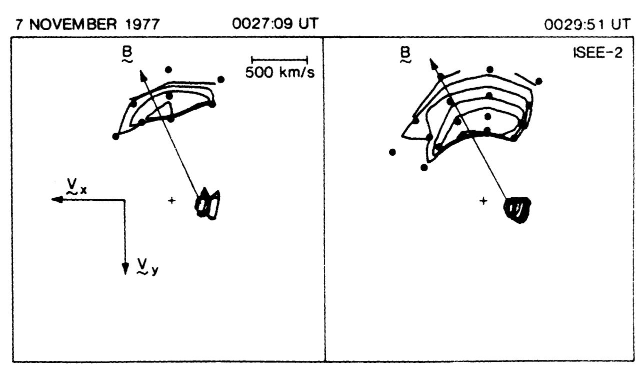

Fig. 2. Three-second snapshots of ion beam distributions measured during the event in Figure 1. Contours of constant two-dimensional phase space density are plotted with one contour for each half decade of phase space density. The innermost closed contours of the beam distribution in the left-hand and right-hand panels correspond to $f(v) = 5.62 \times 10^{-26}$ cm^{-6} s^3 and $f(v) = 5.62 \times 10^{-25}$ cm^{-6} s^3, respectively. The cross in the center of each snapshot identifies zero velocity in the spacecraft frame. Positive V_x and V_y point sunward and duskward, respectively. Solid circles in each snapshot show the actual measurement points where the count rate was above background. The two field-aligned beams have distinct non-Maxwellian characteristics such as a steep slope parallel to the magnetic field and, in the distribution in the right-hand panel, a steep slope strongly oblique to the magnetic field.

velocity space, plotted with one contour for each half decade of phase space density. The vector **B** identifies the ecliptic plane projection of the magnetic field and was determined from 12-s-averaged magnetic field measurements from the University of California, Los Angeles (UCLA), magnetometer on ISEE 2 [*Russell*, 1978]. At the origin of this vector is the solar wind ion distribution, which is not well resolved by the FPE. The ion distribution in the left-hand panel is not associated with enhanced ion acoustic fluctuations, while the one in the right-hand panel is (see Figure 1).

In this paper we will use the term "integrated temperature" to denote a temperature numerically derived from the second velocity moment of the beam distribution. In the left- and right-hand panels of Figure 2 the integrated temperatures are 1×10^7 and 5×10^6 °K, respectively; both of these are much larger than the solar wind ion temperature. However, such a temperature cleary does not fully describe such distinctly non-Maxwellian distributions as those shown in Figure 2. The closely spaced contours on the solar wind side and parallel to **B** indicate a steep slope on that side. Furthermore, the beam in the right-hand panel may have a steep slope in a direction strongly oblique to the magnetic field. The effective temperatures of these edges by themselves are much lower than the temperatures obtained by integrating over the entire beam distributions.

We cannot quantify the cold temperatures strongly oblique to the magnetic field because of the coarseness of the azimuthal sampling of the FPE. The FPE samples every 22.5° in azimuth with a ±4° azimuthal instrument response [*Bame et al.*, 1978]. Thus very cold temperatures $T_{\perp b} \simeq T_c$ of a few times 10^4 °K are not resolved with the FPE. Unfortunately, these are the temperatures needed for instability of the ion acoustic mode [see *Gary and Omidi*, 1986, Figure 7].

Theory

In this section we consider the linear theory of the ion/ion acoustic instability in a homogeneous Vlasov plasma. The plasma configuration consists of three components: Maxwellian electrons (denoted by subscript *e*) and two bi-Maxwellian ion components, a more dense core representing the solar wind ions (subscript *c*), and a less dense beam (subscript *b*) with beam-core relative drift $\mathbf{v}_0$ along the ambient magnetic field $\mathbf{B}_0$.

Our concern is with ion-acustic-like fluctuations which are observed to be primarily electrostatic, so that we consider the electrostatic dispersion equation. The properties of the ion/ion acoustic instability in the electrostatic approximation have been reviewed in detail by *Gary and Omidi* [1986]; here we simply summarize several of their results as they pertain to ion beams in the upstream region.

A relative streaming between two ion components with $\mathbf{v}_0 \times \mathbf{B}_0 = 0$ can drive both the electron/ion acoustic and the ion/ion acoustic instability. At $n_b \ll n_c$ and $v_0 \leq v_e$, both instabilities satisfy the ion acoustic dispersion equation

$$\omega_r = kc_s \qquad k\lambda_{De} \ll 1$$

where

$$c_s \equiv \left(\frac{T_e + 3T_c}{m_c}\right)^{1/2}$$

The ion/ion acoustic instability has a cutoff value of T_e/T_c which is a function of T_b/T_c and n_b/n_e; below this value the mode is stable for all values of the beam-core relative drift speed. If T_e/T_c exceeds this cutoff, the ion/ion instability has a much lower threshold v_0 than its electron/ion counterpart. Near threshold drift speed the ion/ion acoustic instability has maximum growth rate at $\mathbf{k} \times \mathbf{B}_0 = 0$, but as the beam-core relative drift speed is increased, the maximum growth rate shifts to propagation oblique to the magnetic field and the mode becomes stabilized at parallel propagation, in contrast to the electron/ion acoustic instability. At $T_b/T_c \ll 1$, appropriate for ion beams in the plasma sheet boundary layer [*Grabbe and Eastman*, 1984], the ion/ion acoustic instability is nonresonant, but at $T_b/T_c \geq 1$, as is the case for field-aligned beams upstream from the bow shock, this mode becomes beam resonant [*Gary and Omidi*, 1986, Figure 4] so that velocity space details of the ion beam distribution become important for determining instability growth rates.

Figure 3 illustrates the two-dimensional ion distribution function for two Maxwellian distributions with relative drift, and associated properties of the ion/ion acoustic instability at maximum growth rate. Since $v_0 \gg c_s$ here, the wave vector **k** (denoted by the arrows) is strongly oblique to both $\mathbf{B}_0$ and $\mathbf{v}_0$ ($= \mathbf{v}_{0b} - \mathbf{v}_{0c}$). The dashed lines represent velocities which satisfy the Landau resonance condition $\omega_r = \mathbf{k} \cdot \mathbf{v}$ and which most strongly contribute to γ. These lines lie relatively far out on the flanks of the core distribution, so that the instability is nonresonant with respect to this component. In contrast, the dashed lines intersect the flanks of the beam component well into the thermal part of the distribution, so that the instability is beam resonant. Furthermore, since $\gamma \gg \Omega_i$, the ion response to the fluctuating fields is unmagnetized [*Gary and Omidi*, 1986, appendix], so that as long as $\gamma \ll \omega_r$, the positive contribution to the growth rate is proportional to the slope of the beam distribution in the direction of **k**. Thus a steepening of the velocity distribution along the flanks of the beam is the velocity space property which is necessary to drive the ion/ion acoustic instability more strongly and thereby reduce the T_e/T_c cutoff of this mode.

Although we have not constructed a dispersion equation based on the strongly non-Maxwellian distributions of Figure 2, we have used the bi-Maxwellian capabilities of the dispersion code used by *Gary and Omidi* [1986] to illustrate this

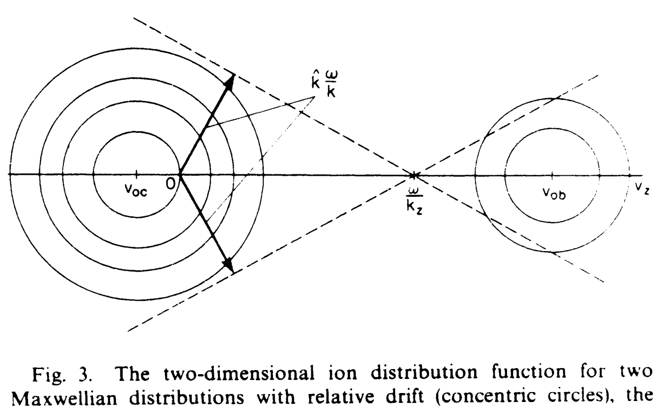

Fig. 3. The two-dimensional ion distribution function for two Maxwellian distributions with relative drift (concentric circles), the two-dimensional phase speed vectors of the ion/ion acoustic instability at maximum growth rate (arrows), and the two-dimensional velocity resonance cone corresponding to $\omega_r = \mathbf{k} \cdot \mathbf{v}$ (dashed lines). The parameters used here are $T_c = T_b = T_i$, $T_e = 10T_i$, $n_b = 0.10n_e$, and $v_0 = 10v_i$, which corresponds to maximum growth rate at $k = 0.17k_i$, $\omega_r = 0.46\omega_i$, and $\vartheta = 61°$.

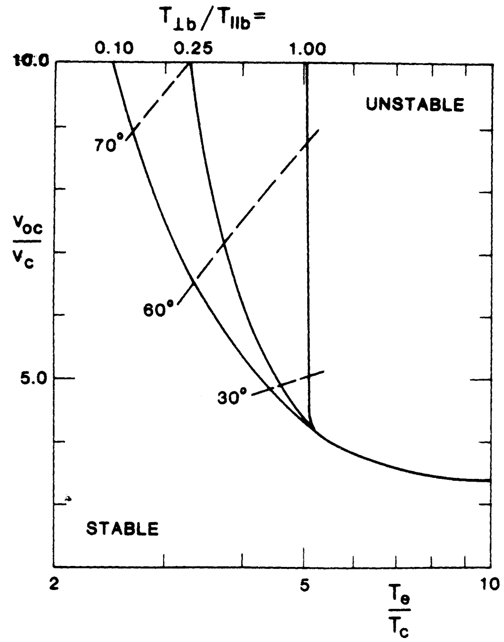

Fig. 4. The threshold core drift speed for the ion/ion acoustic instability as a function of T_e/T_c for three different values of $T_{\perp b}/T_{\parallel b}$. The solid lines represent v_{0c}/v_c at threshold, and the dashed lines indicate the value of ϑ at which the instability arises. Parameters here are $m_c = 1836 m_e$, $n_b = 0.10 n_e$, and $T_b = T_c = T_i$. These results are obtained from the electrostatic dispersion equation for unmagnetized components (compare Figure 2 of *Akimoto and Winske* [1985]).

point. To enhance the steepness of the flanks of the beam distribution artificially, one may reduce $T_{\perp b}/T_{\parallel b}$ below unity while holding $T_{\parallel b}/T_{\parallel c}$ constant. Figure 4 displays the results of ion/ion acoustic instability thresholds calculated under such a beam anisotropy reduction. (This figure is an extension of the work of *Akimoto and Winske* [1985], who considered $T_{\perp b}/T_{\parallel b} > 1.0$.) At $T_{\perp b}/T_{\parallel b} = 1$, the plot of threshold v_{0c} versus T_e/T_c shows an electron temperature cutoff: the vertical line implies that the ion/ion acoustic instability cannot grow at any beam-core relative drift speed below $T_e/T_c = 5.1$. However, as $T_{\perp b}/T_{\parallel b}$ is reduced and the flanks of the beam distribution become steeper, the instability may grow at successively smaller values of T_e/T_c. Note that as T_e/T_c is reduced below 5.1, the instability threshold is no longer at $\vartheta = 0°$, but at successively more oblique propagation angles relative to $\mathbf{B}_0$.

Discussion

If we use the average parameters quoted by *Thomsen* [1985] for field-aligned beams upstream from the bow shock and representative solar wind electron temperatures, we have

$$n_b \simeq 0.01 n_e \qquad T_b \gg T_c \qquad T_e = (1\text{–}7) T_c$$

With these parameters a plasma with Maxwellian distributions is quite stable to the ion/ion acoustic instability. In order that this instability may grow, large changes in one or more of these parameters are needed. *Gary and Omidi* [1986] have suggested that one way of achieving this is that the effective beam temperature in the resonant region of velocity space be significantly lower than the integrated beam temperature. As noted above, steep regions in velocity space apparently exist in observed field-aligned beams such as that shown in the right-hand panel of Figure 2. Velocity space contours from other upstream ion beam events also show the suggestion of steep regions in velocity space.

We have not done a detailed analysis of the beam event in Figures 1 and 2 because of the coarseness of the velocity space sampling of the instrument. The FPE samples velocity space every 22.5° in azimuth with an azimuthal response of approximately ±4°. To resolve the very cold effective temperatures that would be needed for instability ($T_{\perp b} \sim T_c \sim 10^4$ °K) would require an azimuthal resolution of the order of 1°. Because of these instrument limitations we can only suggest and not quantitatively confirm that the non-Maxwellian edge of the distribution is sufficient to drive the ion/ion acoustic instability.

In this paper we have proposed an explanation for the source of enhanced ion acoustic fluctuations observed in association with the relatively cold field-aligned ion beams. Ion acoustic fluctuations are also known to be associated with diffuse distributions [*Anderson et al.*, 1981]. This presents a difficulty in that diffuse distributions are believed to be produced by pitch angle scattering and eventual disruption of field-aligned beams [*Gary et al.*, 1981]. Because pitch angle scattering will destroy any steep perpendicular slope of a beam distribution, it is difficult to see how to extend the present work to the ion acoustic fluctuations associated with diffuse distributions.

Summary

Previous observations have demonstrated a general correlation between suprathermal ions and enhanced ion acoustic fluctuations upstream from the earth's bow shock. However, observations reported here show that on fine time scales the ion acoustic fluctuations are bursty and not well correlated with field-aligned ion beam density changes (cf. Figure 1). This lack of correlation suggests that velocity space details of the ion beam distribution determine instability of the ion acoustic mode. The ion beam distributions shown in Figure 2 display potential free energy sources in the form of steep slopes parallel and possibly strongly oblique to the magnetic field. At the high drift speeds ($v_0 \gg c_s$) characteristic of field-aligned ion beams in the upstream region, the velocity space property of the beam which is conducive to the generation of the ion/ion acoustic instability is the steep slope strongly oblique to the magnetic field (see Figure 3). We therefore suggest that it is such steep sides of the field-aligned beams which give rise to the observed ion acoustic fluctuations. Although velocity space contours of other upstream ion beams show the possibility of steep slopes strongly oblique to the magnetic field, we cannot confirm that this feature gives rise to the ion acoustic fluctuations because of instrument sampling limitations.

Acknowledgments. The ISEE 1 and 2 fast plasma experiments are the result of a collaboration between Los Alamos National Laboratory and the Max-Planck-Institut für extraterrestrische Physik, Garching. G. Paschmann is the principal investigator for the ISEE 2 FPE. Magnetic field data used in this study were obtained by the ISEE 1 and 2 flux gate magnetometers (C. T. Russell, principal investigator) and were provided by the National Space Science Data Center. This work was performed under the auspices of the U.S. Department of Energy and was supported by the DOE Office of Basic Energy Sciences, Geosciences, as well as the NASA Solar Terrestrial Theory Program (Los Alamos), NASA grant S-D4039-D, and the Los Alamos National Laboratory Director's postdoctoral program. Research at the University of Iowa is supported by NASA grant NGL 16-001-043.

The Editor thanks M. K. Hudson and J. LaBelle for their assistance in evaluating this paper.

REFERENCES

Akimoto, K., and D. Winske, Ion-acoustic-like waves excited by the reflected ions at the earth's bow shock, *J. Geophys. Res.*, *90*, 12,095, 1985.

Anderson, R. R., G. K. Parks, T. E. Eastman, D. A. Gurnett, and L. A. Frank, Plasma waves associated with energetic particles streaming into the solar wind from the earth's bow shock, *J. Geophys. Res.*, *86*, 4493, 1981.

Bame, S. J., J. R. Asbridge, H. E. Felthauser, J. P. Glore, G. Paschmann, P. Hemmerich, K. Lehmann, and H. Rosenbauer, ISEE-1 and ISEE-2 fast plasma experiment and the ISEE-1 solar wind experiment. *IEEE Trans. Geosci. Electron.*, *GE-16*, 216, 1978.

Fuselier, S. A., and D. A. Gurnett, Short wavelength ion waves upstream of the earth's bow shock, *J. Geophys. Res.*, *89*, 91, 1984.

Gary, S. P., and N. Omidi, The ion/ion acoustic instability, *J. Plasma Phys.*, in press, 1986.

Gary, S. P., J. T. Gosling, and D. W. Forslund, The electromagnetic ion beam instability upstream of the earth's bow shock, *J. Geophys. Res.*, *86*, 6691, 1981. (Correction, *J. Geophys. Res.*, *89*, 404, 1984.)

Grabbe, C. L., New results on the generation of broadband electrostatic waves in the magnetotail, *Geophys. Res. Lett.*, *12*, 483, 1985.

Grabbe, C. L., and T. E. Eastman, Generation of broadband electrostatic noise by ion beam instabilities in the magnetotail, *J. Geophys. Res.*, *89*, 3865, 1984.

Grard, R., A. Pedersen, J.-G. Trotignon, C. Beghin, M. Mogilevsky, Y. Mikhailov, O. Molchanov, and V. Formisano, Observations of waves and plasm in the environment of comet Halley, *Nature*, *321*, 290, 1986.

Gurnett, D. A., Plasma waves and instabilities, in *Collisionless Shocks in the Heliosphere: Reviews of Current Research*, *Geophys. Monogr. Ser.*, vol. 35, edited by B. T. Tsurutani and R. G. Stone, p. 207, AGU, Washington, D. C., 1985.

Gurnett, D. A., and R. R. Anderson, Plasma wave electric fields in the solar wind: Initial results from Helios 1, *J. Geophys. Res.*, *82*, 632, 1977.

Gurnett, D. A., and L. A. Frank, Ion acoustic waves in the solar wind, *J. Geophys. Res.*, *83*, 58, 1978.

Gurnett, D. A., F. L. Scarf, R. W. Fredricks, and E. J. Smith, The ISEE-1 and ISEE-2 plasma wave investigation, *IEEE Trans. Geosci. Electron.*, *GE-16*, 225, 1978.

Gurnett, D. A., E. Marsch, W. Pilipp, R. Schwenn, and H. Rosenbauer, Ion acoustic waves and related plasma observations in the solar wind, *J. Geophys. Res.*, *84*, 2029, 1979*a*.

Gurnett, D. A., F. M. Neubauer, and R. Schwenn, Plasma wave turbulence associated with an interplanetary shock, *J. Geophys. Res.*, *84*, 541, 1979*b*.

Kennel, C. F., F. L. Scarf, F. V. Coroniti, E. J. Smith, and D. A. Gurnett, Nonlocal plasma turbulence associated with interplanetary shocks, *J. Geophys. Res.*, *87*, 17, 1982.

Omidi, N., Broadband electrostatic noise produced by ion beams in the earth's magnetotail, *J. Geophys. Res.*, *90*, 12,330, 1985.

Rodriguez, P., Magnetosheath electrostatic turbulence, *J. Geophys. Res.*, *84*, 917, 1979.

Russell, C. T., The ISEE-1 and -2 fluxgate magnetometers, *IEEE Trans. Geosci. Electron.*, *GE-16*, 239, 1978.

Scarf, F. L., R. W. Fredricks, L. A. Frank, C. T. Russell, P. J. Coleman, Jr., and M. Neugebauer, Direct correlations of large-amplitude waves with suprathermal protons in the upstream solar wind, *J. Geophys. Res.*, *75*, 7316, 1970.

Scarf, F. L., R. W. Fredricks, L. A. Frank, and M. Neugebauer, Nonthermal electrons and high-frequency waves in the upstream solar wind, 1, Observations, *J. Geophys. Res.*, *76*, 5162, 1971.

Scarf, F. L., F. V. Coroniti, C. F. Kennel, E. J. Smith, J. A. Slavin, B. T. Tsurutani, S. J. Bame, and W. C. Feldman, Plasma wave spectra near slow mode shocks in the distant magnetotail, *Geophys. Res. Lett.*, *11*, 1050, 1984.

Scarf, F. L., F. V. Coroniti, C. F. Kennel, D. A. Gurnett, W.-H. Ip, and E. J. Smith, Plasma wave observations at comet Giacobini-Zinner, *Science*, *232*, 377, 1986.

Thomsen, M. F., Upstream suprathermal ions, in *Collisionless Shocks in the Heliosphere: Reviews of Current Research*, *Geophys. Monogr. Ser.*, vol. 35, edited by B. T. Tsurutani and R. G. Stone, p. 253, AGU, Washington, D. C., 1985.

Thomsen, M. F., H. C. Barr, S. P. Gary, W. C. Feldman, and T. E. Cole, Stability of electron distributions within the earth's bow shock, *J. Geophys. Res.*, *88*, 3035, 1983.

S. J. Bame, S. P. Gary, and M. F. Thomsen, Los Alamos National Laboratory, ESS-8, MS D438, Los Alamos, NM 87545.

S. A. Fuselier, Lockheed Palo Alto Research Laboratory, 3251 Hanover Street, Building 255, Department 91-20, Palo Alto, CA 94304.

D. A. Gurnett, Department of Physics and Astronomy, University of Iowa, Iowa City, IA 52242.

(Received September 2, 1986;
revised February 3, 1987;
accepted February 5, 1987.)